CHINESE OPTICS LETTERS

Vol. 20, No. 6 | June 2022

Three methods for the single-photon transport in a chiral cavity quantum electrodynamics system

Jiang-Shan Tang (唐江山)[1,2,†], Lei Tang (唐 磊)[1,†], and Keyu Xia (夏可宇)[1,2,*]

[1] College of Engineering and Applied Sciences, National Laboratory of Solid State Microstructures, and Collaborative Innovation Center of Advanced Microstructures, Nanjing University, Nanjing 210023, China

[2] School of Physics, Nanjing University, Nanjing 210023, China

*Corresponding author: keyu.xia@nju.edu.cn

Received January 25, 2022 | Accepted March 25, 2022 | Posted Online April 27, 2022

We investigate the single-photon transport problem in the system of a whispering-gallery mode microresonator chirally coupled with a two-level quantum emitter (QE). Conventionally, this chiral QE-microresonator coupling system can be studied by the master equation and the single-photon transport methods. Here, we provide a new approach, based on the transfer matrix, to assess the single-photon transmission of such a system. Furthermore, we prove that these three methods are equivalent. The corresponding relations of parameters among these approaches are precisely deduced. The transfer matrix can be extended to a multiple-resonator system interacting with two-level QEs in a chiral way. Therefore, our work may provide a convenient and intuitive form for exploring more complex chiral cavity quantum electrodynamics systems.

Keywords: chiral cavity QED system; master equation method; single-photon transport theory; transfer matrix method.
DOI: 10.3788/COL202220.062701

1. Introduction

The interaction of light and matter at the single-quantum level is the basis of essential physics of many phenomena and applications[1], which has been extensively explored in various quantum systems, such as quantum emitters (QEs) coupling with single-mode waveguides[2–9], cavities[10–18], plasmons[19–23], and whispering-gallery mode microresonators[24–30]. In recent years, an emerging field of research, called "chiral quantum optics"[31], exhibits chiral interactions of light and QEs[32–38] and has received extensive attention in the field of optical nonreciprocity[32,35,39–41].

To realize the chiral light–matter interaction, an external magnetic field is usually required to induce the magneto-optical effect[41] or initialize the states of QEs[42]. It greatly limits the miniaturization and integration of single-photon devices. Recently, all-optical approaches, based on the optical Stark shift of quantum dots (QDs)[35] and the valley-selective response in transition metal dichalcogenides[43], have been proposed to release the requirement of magnetic biases. Towards on-chip chiral single-photon interfaces, non-magnetic schemes have been designed based on a whispering-gallery mode microresonator chirally coupled with a two-level QE[32,35,39,40].

Theoretically, the single-photon transport (SPT) problem in the system of a whispering-gallery mode microresonator coupled to a waveguide can be solved by methods such as the master equation (ME)[44–49], the SPT[4,26,50–52], and the transfer matrix (TM)[53]. The whispering-gallery mode microresonator system containing a two-level QE has also been discussed under the framework of the ME and SPT theory[4,24,26,54], even extending to the chiral interactions[31,32,35,40]. However, how to deal with the chiral interaction of a whispering-gallery mode microresonator with a two-level QE using the TM method is still not available. The inner link among these three methods also remains to be revealed.

In this work, we study the SPT problem in a chiral QE-microresonator system using the TM method. By introducing a nonlinear coefficient related to the two-level QE into the transfer relation, we can use the TM method to solve the single-photon transmission. In this sense, the two-level QE can be regarded as a single-photon phase-amplitude modulator. Furthermore, we demonstrate that the ME, SPT, and TM methods are equivalent in dealing with such chiral cavity quantum electrodynamics (QED) systems. The correspondence between the parameters of the three methods is strictly deduced.

This paper is organized as follows. In Sec. 2, we review the ME and the SPT theory for the SPT problem in a chiral QE-microresonator system, respectively. Next, we discuss the TM approach and show that the three methods above are equivalent if we treat the two-level QE as a single-photon phase-amplitude modulator. In Sec. 3, we show the numerical results of these three methods. In the end, we present a conclusion in Sec. 4.

2. System and Model

The chiral QE-microresonator system, depicted in Fig. 1, consists of a whispering-gallery mode microresonator, a waveguide, and a two-level QE. The microresonator, which can be made with various material platforms, such as silicon oxynitride[55,56], polymers[57], or silicon on insulator[58–60], supports two traveling wave modes, i.e., clockwise (CW) and counterclockwise (CCW) modes. Near the outer sidewall of the microresonator, the evanescent fields of the whispering-gallery modes are almost perfectly circularly polarized with its polarization locked to the propagation direction[27,35]. We assume that the evanescent field of the CCW mode is σ^+-polarized and that of the CW mode is σ^--polarized. As shown in Fig. 1, the QE is positioned near the outer sidewall of the microresonator. After initializing the QE in a specific spin ground state[61–63] or shifting the transition energy with a polarization-selective optical Stark effect[64–66], we can treat the QE as a two-level system with only σ^+-polarization-driven transition. One can use a precisely positioned atom[40,67], QD[34,42,68,69], or nanopillar covered by monolayers[70–72] to construct that two-level QE. As a result, the QE-microresonator coupling strength is dependent on the propagating direction of light in our chiral system. In the forward case, the incident light from port 1 excites the CCW mode, and it strongly couples with the QE with the coupling strength g. However, in the backward (port 2 incident) case, the CW mode is decoupled with the QE, and thus the coupling rate is negligible (i.e., $g \approx 0$). Practically, backscattering is usually present due to the surface roughness of the microresonator. In this paper, we treat the backscattering as one scatterer[73], as depicted in Fig. 1.

Below, we first provide the ME, SPT, and TM methods to solve the response of the system. Then, we show that these three methods are equivalent if we treat the two-level QE as a single-photon phase-amplitude modulator. We only discuss the forward case ($g \neq 0$) in detail, and the backward case corresponds to the system without the QE ($g = 0$).

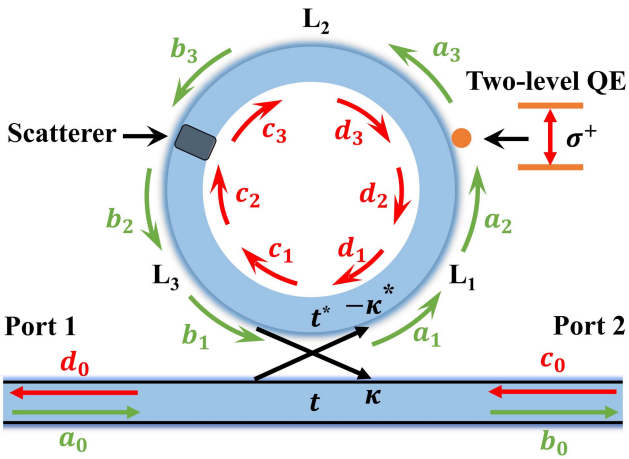

Fig. 1. Schematic of a chiral QE-microresonator system. A two-level QE is coupled to a whispering-gallery mode microresonator in a chiral way to form the QE-microresonator system. A waveguide is side coupled to the microresonator as input and output ports. A scatterer on the microresonator is considered to introduce backscattering. The arrows represent the propagating direction of a single photon for an input to port 1 (green) or port 2 (red).

2.1. Master Equation Method

In this section, we discuss the ME method to solve our model. For a coupled atom-microresonator system, it has been analyzed[24]. Here, we discuss the chiral coupling using the same approach. We consider that a two-level QE with transition frequency ω_{qe} is coupled to the CCW mode and decoupled to the opposite mode. The two degenerate whispering-gallery modes, with same resonant frequency Ω and dissipation κ_{tol}, are assumed to be coupled with each other in a strength h due to the scatterer. Here, we divide the dissipation κ_{tol} into two parts, the intrinsic decay rate of κ_{in} and the external loss of κ_{ex}, satisfying $\kappa_{tol} = \kappa_{in} + \kappa_{ex}$. A weak coherent field of frequency ω with an amplitude α_{in} drives the CCW mode a. In a good single-photon approximation, $\alpha_{in} \ll 1$. In a frame rotating at the frequency ω, the Hamiltonian of our system can be obtained[74]:

$$H = -\Delta_1 a^\dagger a - \Delta_2 \sigma^+\sigma^- - \Delta_1 b^\dagger b + i\sqrt{2\kappa_{ex}}\alpha_{in}(a^\dagger - a) + g(a^\dagger\sigma^- + \sigma^+ a) + h(a^\dagger b + b^\dagger a), \tag{1}$$

where g represents the coupling strength between the CCW mode and the QE. $\Delta_1 = \omega - \Omega$ and $\Delta_2 = \omega - \omega_{qe}$ are the detunings. b is the annihilation operator of the CW mode. $\sigma^\pm$ are the raising and lowering operators describing the two-level QE. It is worth noting that if we consider the coupling of two microresonators instead of the scatterer, the Hamiltonian has the same form as Eq. (1). In this case, h describes the coupling strength between the two microresonators.

Introducing the dissipation of the QE, γ, the evolution of the system can be found by solving the ME,

$$\dot{\rho} = -i[H,\rho] + \kappa_{tol}(2a\rho a^\dagger - a^\dagger a\rho - \rho a^\dagger a) + \kappa_{tol}(2\,b\rho b^\dagger - b^\dagger b\rho - \rho b^\dagger b) + \gamma(2\sigma^-\rho\sigma^+ - \sigma^+\sigma^-\rho - \rho\sigma^+\sigma^-), \tag{2}$$

where ρ is the density operator. From Eq. (2), we can derive the equations of motion,

$$\dot{a} = i\tilde{\Delta}_1 a + \alpha_{in}\sqrt{2\kappa_{ex}} - ig\sigma^- - ihb, \tag{3a}$$

$$\dot{\sigma}^- = i\tilde{\Delta}_2\sigma^- + ig\sigma_z a, \tag{3b}$$

$$\dot{b} = i\tilde{\Delta}_1 b - iha, \tag{3c}$$

and obtain the steady-state solution,

$$\langle a\rangle = \frac{i\alpha_{in}\sqrt{2\kappa_{ex}}\tilde{\Delta}_1\tilde{\Delta}_2}{\tilde{\Delta}_1(\tilde{\Delta}_1\tilde{\Delta}_2 + \langle\sigma_z\rangle g^2) - \tilde{\Delta}_2 h^2}, \tag{4}$$

where $\sigma_z = \sigma^+\sigma^- - \sigma^-\sigma^+$, $\tilde{\Delta}_1 = \Delta_1 + i\kappa_{tol}$, and $\tilde{\Delta}_2 = \Delta_2 + i\gamma$. According to the input–output relation, $\langle a_{out}\rangle = \alpha_{in} - \sqrt{2\kappa_{ex}}\langle a\rangle$,

the transmission amplitude is defined as $t_\omega = \langle a_{\rm out}\rangle/\alpha_{\rm in}$. Thus, we can get the transmission amplitude in port 2:

$$t_\omega = \frac{\tilde{\Delta}_1[(\Delta_1 + i\kappa_{\rm in} - i\kappa_{\rm ex})\tilde{\Delta}_2 + \sigma_z g^2] - \tilde{\Delta}_2 h^2}{\tilde{\Delta}_1(\tilde{\Delta}_1\tilde{\Delta}_2 + \sigma_z g^2) - \tilde{\Delta}_2 h^2}. \tag{5}$$

The transmission of port 2 can be obtained from $T = |t_\omega|^2$. Moreover, the full quantum dynamics of the system can be found by numerically solving Eq. (2) in a truncated space of photon number for the whispering-gallery modes.

2.2. Single-photon transport method

Hereafter, we consider only a single photon in our system. Based on the SPT theory[4,26,50], our previous work[35] has given a transmission amplitude for such a chiral system. The Hamiltonian for the single-excitation system takes the form[35]

$$\begin{aligned} H = &\int {\rm d}x c_{\rm F}^\dagger(x)\left(\omega_0 - iv_{\rm g}\frac{\partial}{\partial x}\right)c_{\rm F}(x) \\ &+ \int {\rm d}x c_{\rm B}^\dagger(x)\left(\omega_0 + iv_{\rm g}\frac{\partial}{\partial x}\right)c_{\rm B}(x) \\ &+ (\Omega - i\kappa_{\rm in})a^\dagger a + (\Omega - i\kappa_{\rm in})b^\dagger b \\ &+ (\Omega_{\rm e} - i\gamma)a_{\rm e}^\dagger a_{\rm e} + \Omega_{\rm g} a_{\rm g}^\dagger a_{\rm g} \\ &+ \int {\rm d}x\delta(x)\left[V_{\rm a}c_{\rm F}^\dagger(x)a + V_{\rm a}^* a^\dagger c_{\rm F}(x)\right] \\ &+ \int {\rm d}x\delta(x)\left[V_{\rm b}c_{\rm B}^\dagger(x)b + V_{\rm b}^* b^\dagger c_{\rm B}(x)\right] \\ &+ ga\sigma_+ + g^* a^\dagger\sigma_- + hb^\dagger a + h^* a^\dagger b, \end{aligned} \tag{6}$$

where $c_{\rm F/B}^\dagger(x)$ is a Bosonic operator creating a forward- or backward-moving photon with reference frequency ω_0 at x in the waveguide, $\sigma^+ = a_{\rm e}^\dagger a_{\rm g}$ ($\sigma^- = a_{\rm g}^\dagger a_{\rm e}$) is the raising (lowering) operator for the QE with transition frequency $\omega_{\rm qe} = \Omega_{\rm e} - \Omega_{\rm g}$, g is the coupling strength for the interaction between the QE and the CCW mode a, and the QE is decoupled to the CW mode b in our system. $V_{\rm a/b}$ is the waveguide-microresonator coupling strength of mode a or b. We set $V_{\rm a} = V_{\rm b} = V$ and thus have the external decay rate of the microresonator $\kappa_{\rm ex} = V^2/2v_{\rm g}$, where $v_{\rm g}$ is the group velocity of the photon in the waveguide.

A single-excitation state for the system is given by

$$\begin{aligned} |\psi\rangle = &\int {\rm d}x[\tilde{\varphi}_{\rm F}(x,t)c_{\rm F}^\dagger(x) + \tilde{\varphi}_{\rm B}(x,t)c_{\rm B}^\dagger(x)]|\varnothing\rangle \\ &+ [\tilde{e}_{\rm a}(t)a^\dagger + \tilde{e}_{\rm b}(t)b^\dagger + \tilde{e}_{\rm qe}(t)\sigma^+]|\varnothing\rangle, \end{aligned} \tag{7}$$

with the eigenfrequency ω, where $\tilde{\varphi}_{\rm F/B}(x,t)$ is the single-photon wave function of the forward- or backward-moving mode, $\tilde{e}_{\rm a/b}$ is the excitation amplitude of mode a or b, and $\tilde{e}_{\rm qe}$ is the excitation amplitude of the QE. Note that $\Upsilon = e^{-i\omega t}\Upsilon$ with $\Upsilon \in \{\varphi_{\rm R},\varphi_{\rm L},e_{\rm a},e_{\rm b},e_{\rm q}\}$. $|\varnothing\rangle$ is the vacuum state. To solve the single-photon transmission amplitude, we take $\varphi_{\rm F}(x) = e^{iqx}[\theta(-x) + t_\omega\theta(x)]$ and $\varphi_{\rm B}(x) = r_\omega e^{-iqx}\theta(-x)$ with the Heaviside step function $\theta(x)$, where t_ω (r_ω) is the transmission (reflection) amplitude, and q is the wave vector of the input field with the frequency around ω. Based on the Schrödinger equation in real space, $H|\psi\rangle = i\partial|\psi\rangle/\partial t$, we can derive the steady-state transmission amplitude in port 2:

$$t_\omega = \frac{\tilde{\Delta}_1[(\Delta_1 + i\kappa_{\rm in} - i\kappa_{\rm ex})\tilde{\Delta}_2 - g^2] - \tilde{\Delta}_2 h^2}{\tilde{\Delta}_1(\tilde{\Delta}_1\tilde{\Delta}_2 - g^2) - \tilde{\Delta}_2 h^2}, \tag{8}$$

where the detunings Δ_1, $\tilde{\Delta}_1$, and $\tilde{\Delta}_2$ are the same as the parameters in Sec. 2.1.

If we consider $\sigma_z = -1$ in the ME method, that is, the weak probe field approximation[74], we can find that Eq. (5) and Eq. (8) are equivalent. In Sec. 2.4, we will verify that the TM method is consistent with the SPT method.

2.3. Transfer matrix method

Next, we study the chiral QE-microresonator system using the TM method. Under the notation in Fig. 1, the coupling relation between the waveguide and the microresonator can be written as

$$\begin{cases} a_1 = t^* b_1 - \kappa^* a_0 \\ b_0 = t a_0 + \kappa b_1 \end{cases}, \quad \begin{cases} c_1 = t^* d_1 - \kappa^* c_0 \\ d_0 = t c_0 + \kappa d_1 \end{cases}, \tag{9}$$

where t and κ are the transmission and coupling coefficients, and $|t|^2 + |\kappa|^2 = 1$ for lossless coupling. We write Eq. (9) in a matrix form:

$$\begin{aligned} \begin{pmatrix} a_0 \\ b_0 \\ c_0 \\ d_0 \end{pmatrix} &= \frac{1}{\kappa^*}\begin{pmatrix} -1 & t^* & 0 & 0 \\ -t & 1 & 0 & 0 \\ 0 & 0 & -1 & t^* \\ 0 & 0 & -t & 1 \end{pmatrix}\begin{pmatrix} a_1 \\ b_1 \\ c_1 \\ d_1 \end{pmatrix} \\ &\equiv M_{\rm cpl}\begin{pmatrix} a_1 \\ b_1 \\ c_1 \\ d_1 \end{pmatrix}. \end{aligned} \tag{10}$$

The size of the QE and the scatterer is much smaller than that of the structure of the microresonator, so theoretically they can be treated as particles. We assume the coupling point of the waveguide with the microresonator, QE, and scatterer divide the microresonator into three parts with lengths L_j (j = 1, 2, 3), satisfying $L_1 + L_2 + L_3 = 2\pi R$; see Fig. 1. Here, R is the radius of the microresonator. The field component notations are shown in Fig. 1. When a single photon propagates around the microresonator, it will accumulate propagation phases $\theta_j = \beta L_j$ and may attenuate with loss $\alpha_j(L_j)$[53]. We take $\theta = \theta_1 + \theta_2 + \theta_3$ and $\alpha = \alpha_1\alpha_2\alpha_3$. The factor β is the propagation constant in the microresonator as given by $\beta = n_{\rm eff}\omega/c$, where

n_{eff} is the effective refractive index, and ω is the frequency. Thus, we have the transfer relation

$$\begin{pmatrix} a_1 \\ b_1 \\ c_1 \\ d_1 \end{pmatrix} = M_{\text{pro}} M_x \begin{pmatrix} a_3 \\ b_3 \\ c_3 \\ d_3 \end{pmatrix}, \tag{11a}$$

$$b_3 = \alpha_2 e^{i\theta_2} a_3, \tag{11b}$$

$$d_3 = \alpha_2 e^{i\theta_2} c_3, \tag{11c}$$

where

$$M_{\text{pro}} = \begin{pmatrix} \alpha_1^{-1} e^{-i\theta_1} & 0 & 0 & 0 \\ 0 & \alpha_3 e^{i\theta_3} & 0 & 0 \\ 0 & 0 & \alpha_3^{-1} e^{-i\theta_3} & 0 \\ 0 & 0 & 0 & \alpha_1 e^{i\theta_1} \end{pmatrix}, \tag{12}$$

M_x is derived from the contributions of the QE and the scatterer, and its exact form will be discussed below. We refer to M_{cpl} and M_{pro} as coupling and propagation matrices. Combining Eqs. (10) and (11), we obtain the TM as

$$\begin{pmatrix} a_0 \\ b_0 \\ c_0 \\ d_0 \end{pmatrix} = M_{\text{cpl}} M_{\text{pro}} M_x \begin{pmatrix} a_3 \\ b_3 \\ c_3 \\ d_3 \end{pmatrix}. \tag{13}$$

We consider a single input of port 1 ($c_0 = 0$). It excites the CCW-direction whispering-gallery mode. In the following, we will discuss the single-photon transmission in four different cases.

2.3.1. No two-level QE and no scatterer

We first consider the case without two-level QEs and scatterers; the form of M_x can be directly obtained:

$$M_x = \begin{pmatrix} 1 & 0 & 0 & 0 \\ 0 & 1 & 0 & 0 \\ 0 & 0 & 1 & 0 \\ 0 & 0 & 0 & 1 \end{pmatrix}. \tag{14}$$

In the absence of scatterers, the CCW and CW modes are decoupled. Substituting Eq. (14) and Eq. (11) into Eq. (13), we get the transmission amplitude in port 2[53]:

$$t_\omega = \frac{b_0}{a_0} = \frac{-t + \alpha e^{i\theta}}{-1 + \alpha t^* e^{i\theta}}. \tag{15}$$

2.3.2. No two-level QE and one scatterer

In this case, we consider the effect of the scatterer in the microresonator. The relation between the amplitudes can be written as $b_2 = t_s b_3 + r_s c_2$, $c_3 = t_s c_2 + r_s b_3$, $a_3 = a_2$, and $d_2 = d_3$. Thus, we have

$$M_x = \begin{pmatrix} 1 & 0 & 0 & 0 \\ 0 & 1/t_s & r_s/t_s & 0 \\ 0 & -r_s/t_s & 1/t_s & 0 \\ 0 & 0 & 0 & 1 \end{pmatrix}, \tag{16}$$

where t_s and r_s are the transmission and reflection coefficients, respectively. They satisfy $|t_s|^2 + |r_s|^2 = 1$ when the dissipation of the scatterer is neglected. The two whispering-gallery modes are coupled to each other in this case. We assume the scatterer is weak, thus we can write t_s and r_s in the following forms[73]:

$$t_s = \cos\,\varepsilon \approx 1 - \frac{\varepsilon^2}{2}, \quad r_s = i \sin\,\varepsilon \approx i\varepsilon. \tag{17}$$

Then, we have the transmission amplitude in port 2:

$$t_\omega = \frac{b_0}{a_0} = \frac{-t + \alpha e^{i\theta} \frac{t_s - t^* \alpha e^{i\theta}}{1 - t_s t^* \alpha e^{i\theta}}}{-1 + \alpha t^* e^{i\theta} \frac{t_s - t^* \alpha e^{i\theta}}{1 - t_s t^* \alpha e^{i\theta}}}. \tag{18}$$

2.3.3. One two-level QE and no scatterer

Here, we study the effect of a two-level QE directionally coupled to a microresonator. Because the QE is in a specific spin ground state or the polarization-selective energy-level transition, the coupling of the QE and the evanescent field on the microresonator is direction-dependent. The reflection of single-photon propagation will vanish due to such chiral QE–light interaction[32,35]. In this case, the single photon will not excite the CW mode, leading to decoupling between the CCW and CW modes. We assume the single photon through the two-level QE with a transmission coefficient t_{qe}, i.e., $a_3 = t_{\text{qe}} a_2$ and $d_2 = d_3$, such that

$$M_x = \begin{pmatrix} t_{\text{qe}}^{-1} & 0 & 0 & 0 \\ 0 & 1 & 0 & 0 \\ 0 & 0 & 1 & 0 \\ 0 & 0 & 0 & 1 \end{pmatrix}, \tag{19}$$

and

$$t_\omega = \frac{b_0}{a_0} = \frac{-t + \alpha e^{i\theta} t_{\text{qe}}}{-1 + \alpha t^* e^{i\theta} t_{\text{qe}}}. \tag{20}$$

The specific form of t_{qe} will be discussed below.

2.3.4. One two-level QE and one scatterer

Combining with the above discussions, we can obtain the form of M_x, considering both a two-level QE directionally coupled to the microresonator and a scatterer:

$$M_x = \begin{pmatrix} t_{\mathrm{qe}}^{-1} & 0 & 0 & 0 \\ 0 & 1/t_{\mathrm{s}} & r_{\mathrm{s}}/t_{\mathrm{s}} & 0 \\ 0 & -r_{\mathrm{s}}/t_{\mathrm{s}} & 1/t_{\mathrm{s}} & 0 \\ 0 & 0 & 0 & 1 \end{pmatrix}. \tag{21}$$

The transmission amplitude can be calculated as

$$t_\omega = \frac{b_0}{a_0} = \frac{-t + \alpha e^{i\theta} t_{\mathrm{qe}} \frac{t_{\mathrm{s}} - t^* \alpha e^{i\theta}}{1 - t_{\mathrm{s}} t^* \alpha e^{i\theta}}}{-1 + \alpha t^* e^{i\theta} t_{\mathrm{qe}} \frac{t_{\mathrm{s}} - t^* \alpha e^{i\theta}}{1 - t_{\mathrm{s}} t^* \alpha e^{i\theta}}}. \tag{22}$$

It can be found that the transmission amplitude t_ω is independent of the relative distance L_2 between the QE and the scatterer on the microresonator from Eq. (22). This is because the chiral coupling of the QE with the microresonator only causes a modulation of the transmission t_{qe} of the single photon propagating in the microresonator. Such modulation does not depend on the position of the QE on the microresonator; see Eq. (21). Therefore, the case of a single-emitter coupling can be generalized to multi-emitter cases by successively multiplying t_{qe} in the transfer relation of the field amplitudes.

2.4. Single-photon phase-amplitude modulator

We define the round-trip time of the microresonator, $\tau_{\mathrm{rt}} = 2\pi R n_{\mathrm{eff}}/c$, that a photon needs to make a round trip in the microresonator of length $2\pi R$. It is the inverse of the free spectral range $\mathcal{F}$, i.e., $\tau_{\mathrm{rt}} = 1/\mathcal{F}$[75]. Since $\mathcal{F} \gg 1$ for a microresonator, τ_{rt} is a small amount. We have $\exp(i\theta) = \exp[i(\omega - \Omega)\tau_{\mathrm{rt}}] \approx 1 + i\Delta_1\tau_{\mathrm{rt}}$. On the one hand, for a single photon having travelled a round trip in the microresonator, we have $a_1(\tau_{\mathrm{rt}}) = \alpha t^* a_1(0)$ from the transfer relation. The circulating power meets $|a_1(\tau_{\mathrm{rt}})|^2 = \alpha^2 t^2 |a_1(0)|^2$. On the other hand, we can obtain $|a_1(\tau_{\mathrm{rt}})|^2 = \exp(-2\kappa_{\mathrm{tol}}\tau_{\mathrm{rt}})|a_1(0)|^2$ from the dissipative properties of the microresonator. Hence, we have

$$\alpha = e^{-\kappa_{\mathrm{in}}\tau_{\mathrm{rt}}} \approx 1 - \kappa_{\mathrm{in}}\tau_{\mathrm{rt}}, \tag{23a}$$

$$t = e^{-\kappa_{\mathrm{ex}}\tau_{\mathrm{rt}}} \approx 1 - \kappa_{\mathrm{ex}}\tau_{\mathrm{rt}}. \tag{23b}$$

Because the size of the two-level QE is much smaller than that of the bend structure of the microresonator, the interaction between the evanescent field and the QE can be approximated as a waveguide coupling with a two-level QE directionally[32], with a transmission coefficient

$$t_{\mathrm{qe}} = \frac{\omega - \omega_{\mathrm{qe}} + i(\gamma - \Gamma)}{\omega - \omega_{\mathrm{qe}} + i(\gamma + \Gamma)}, \tag{24}$$

where Γ is the decay rate from the QE into the waveguide. Therefore, substituting Eqs. (17), (23), and (24) into Eq. (22) and ignoring the second-order small quantity, we have

$$\begin{aligned} t_\omega &= \frac{-t + \alpha e^{i\theta} t_{\mathrm{qe}} \frac{t_{\mathrm{s}} - t^* \alpha e^{i\theta}}{1 - t_{\mathrm{s}} t^* \alpha e^{i\theta}}}{-1 + \alpha t^* e^{i\theta} t_{\mathrm{qe}} \frac{t_{\mathrm{s}} - t^* \alpha e^{i\theta}}{1 - t_{\mathrm{s}} t^* \alpha e^{i\theta}}} \\ &\approx \frac{\kappa_{\mathrm{ex}}\tau_{\mathrm{rt}} - 1 + (1 - \kappa_{\mathrm{in}}\tau_{\mathrm{rt}} + i\Delta_1\tau_{\mathrm{rt}})\left[\left(1 - \frac{2i\Gamma}{\tilde{\Delta}_2 + i\Gamma}\right)\left(1 + \frac{\varepsilon^2}{i\tilde{\Delta}_1\tau_{\mathrm{rt}} + \varepsilon^2/2}\right)\right]}{-1 + (1 + i\tilde{\Delta}_1\tau_{\mathrm{rt}})\left[\left(1 - \frac{2i\Gamma}{\tilde{\Delta}_2 + i\Gamma}\right)\left(1 + \frac{\varepsilon^2}{i\tilde{\Delta}_1\tau_{\mathrm{rt}} + \varepsilon^2/2}\right)\right]} \\ &\approx \frac{\tilde{\Delta}_1[(\Delta_1 + i\kappa_{\mathrm{in}} - i\kappa_{\mathrm{ex}})\tilde{\Delta}_2 - \Gamma(2/\tau_{\mathrm{rt}} - \kappa_{\mathrm{tol}})] - \tilde{\Delta}_2\frac{\varepsilon^2}{\tau_{\mathrm{rt}}^2}}{\tilde{\Delta}_1[\tilde{\Delta}_1\tilde{\Delta}_2 - \Gamma(2/\tau_{\mathrm{rt}} - \kappa_{\mathrm{tol}})] - \tilde{\Delta}_2\frac{\varepsilon^2}{\tau_{\mathrm{rt}}^2}} \\ &= \frac{\tilde{\Delta}_1[(\Delta_1 + i\kappa_{\mathrm{in}} - i\kappa_{\mathrm{ex}})\tilde{\Delta}_2 - \Gamma(2\mathcal{F} - \kappa_{\mathrm{tol}})] - \tilde{\Delta}_2(\varepsilon \times \mathcal{F})^2}{\tilde{\Delta}_1[\tilde{\Delta}_1\tilde{\Delta}_2 - \Gamma(2\mathcal{F} - \kappa_{\mathrm{tol}})] - \tilde{\Delta}_2(\varepsilon \times \mathcal{F})^2}. \end{aligned} \tag{25}$$

Comparing Eq. (25) with Eq. (8), we can find that if we take

$$(2\mathcal{F} - \kappa_{\mathrm{tol}})\Gamma = g^2, \quad \varepsilon \times F = h, \tag{26}$$

the TM method and the SPT method are consistent. This also proves that the assumption of Eq. (24) is well valid. For a system in which a two-level QE is chirally coupled to the waveguide, the light field interacts with the QE only once, and the decay rate from the QE into the waveguide is Γ. However, when the QE is coupled to the microresonator, the photons in the microresonator interact with the QE many times. As a result, the microresonator has a feedback modulation to the decay rate Γ. If we define $\Gamma_{\mathrm{eff}} = \sqrt{(2\mathcal{F} - \kappa_{\mathrm{tol}})\Gamma}$, then the physical meaning of Γ_{eff} is the effective decay rate from the QE into the microresonator. It is equal to the coupling strength g. For the second term in Eq. (26), ε is a dimensionless parameter in the TM method. It is equal to the backscattering strength h by multiplying the free spectral range $\mathcal{F}$, which has a dimension of frequency. Note that ε only needs to vary from 0 to π; see Eq. (17). Thus, ε reflects the normalized magnitude of backscattering strength in the microresonator.

Note that the chiral coupling of the two-level QE to the microresonator does not require additional auxiliary fields. This vacuum-induced interaction causes a phase shift and an amplitude modulation of a single photon passing through the QE. Therefore, the two-level QE can be treated as a single-photon phase-amplitude modulator. We divide Eq. (24) into two parts:

$$t_{\mathrm{qe}} = \exp(i\varphi_{\mathrm{pha}})\exp(-\varphi_{\mathrm{dis}}), \tag{27}$$

where $\exp(i\varphi_{\mathrm{pha}}) = \arg(t_{\mathrm{qe}})$ represents the change of the phase, and $\exp(-\varphi_{\mathrm{dis}}) = |t_{\mathrm{qe}}|$ describes the attenuation of the amplitude. The additional propagation phase introduced by the two-level QE can be equivalent to a shift of the effective resonance frequency of the microresonator. When a single photon travels around the microresonator, in the absence of the QE, we have $\theta = 2\pi R\beta = 2\pi m\omega/\Omega$, where $m = \Omega n_{\mathrm{eff}} R/c$ is the

modal number. But, if we consider the chiral QE-microresonator interaction, the additional propagation phase $\varphi_{\rm pha}$ leads to $\theta + \varphi_{\rm pha} = 2\pi m\omega/\Omega_{\rm eff}$. The effective resonance frequency of the microresonator is

$$\Omega_{\rm eff} \approx \Omega\left(1 - \frac{\varphi_{\rm pha}\Omega}{2\pi m\omega}\right), \tag{28}$$

and $\Omega_{\rm eff} \approx \Omega(1 - \varphi_{\rm pha}/2\pi m)$ for $\Omega/\omega \approx 1$.

In general, by equating a two-level QE directionally coupled with a microresonator to a single-photon phase-amplitude modulator, we can use the TM method to solve the SPT problem in such chiral QE-microresonator systems. This only needs to be multiplied by a transmission coefficient $t_{\rm qe}$ in the transfer relation. Furthermore, this approach can be extended to more complex systems such as a coupled-resonator optical waveguide interacting with an array of two-level QEs in a chiral way[76].

3. Results

Below, we numerically study our system to prove the consistency of these three methods. For the TM and SPT methods, we solve Eqs. (22) and (8) directly, whereas, for the ME method, we perform a full quantum dynamics simulation using Eq. (2). We set a prepared QD as the two-level QE for coupling to a silicon-based microresonator in a chiral way. In Figs. 1–4, the experimentally available parameters are chosen as[60,68,77] $R = 10.5\,\mu$m, $n_{\rm eff} = 1.5$, $\mathcal{F}/2\pi = 3$ THz, $\alpha_{\rm in}/\sqrt{\kappa_{\rm tol}} = 0.1$, and $\gamma/2\pi = 6$ MHz. The conversion relationships between the parameters of the three methods are given by Eqs. (23) and (26). We take $t = \alpha = 0.99$, thus satisfying the critical coupling condition, $\kappa_{\rm ex}/2\pi = \kappa_{\rm in}/2\pi = 30$ GHz. The frequency of the QD is resonant with the microresonator, i.e., $\omega_{\rm qe} = \Omega$.

We first consider the case without a two-level QD, corresponding to $\Gamma = 0$ ($g = 0$), shown in Fig. 2. When the strength $h = 0$, the deep transmission appears at the resonance point [see Fig. 2(a)]. As the strength h increases, the transmission spectrum gradually splits [see Figs. 2(b) and 2(c)]. The calculation results of the three methods are exactly the same.

Then, we consider the chiral coupling of a two-level QD. By modeling the two-level QD chirally coupled to the microresonator as a single-photon phase-amplitude modulator, we can use the TM method to solve SPT problems. Figure 3 shows the transmission spectra without scatterers. The presence of the two-level QD causes the transmission spectrum to split[35]. We can find that the transmission spectra calculated by the three methods are consistent regardless of whether it is under weak coupling, $\Gamma = 0.1\gamma$ and $\Gamma = \gamma$ ($g/\kappa_{\rm tol} = 0.03$ and $g/\kappa_{\rm tol} = 0.1$), or strong coupling, $\Gamma = 100\gamma$ ($g/\kappa_{\rm tol} = 1$). The results taking into account the effect of backscattering are shown in Fig. 4. We consider the case of strong coupling, $\Gamma = 100\gamma$. Whether it is in the case of weak backscattering [see Fig. 4(a)] or strong backscattering [see Fig. 4(b)], the calculation results are consistent. Therefore, our numerical results further confirm the above theoretical analyses and prove the correctness of the parameter correspondence among these three methods.

We now discuss the effect of the pump power in the ME method. It is proportional to the driving amplitude $\alpha_{\rm in}$. As we have analyzed above, the three methods are equivalent only if the probe field is a weak pump. It can be found that with the increase of the driving amplitude, the results of the TM method gradually have a difference with those of the ME method,

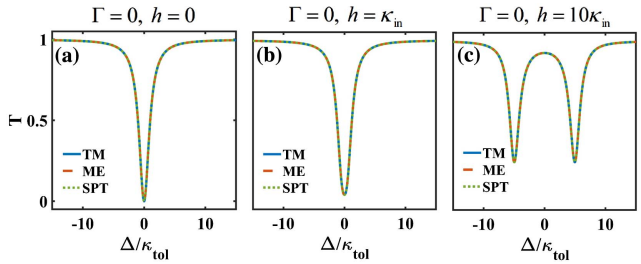

Fig. 2. Transmission spectra of a waveguide coupled with a microresonator. The blue solid, red dashed, and green dotted curves are calculated by the TM, ME, and SPT methods, respectively. The settings in the following figures are the same: (a) in the absence of backscattering, (b) and (c) in presence of the backscattering with strengths $h = \kappa_{\rm in}$ and $h = 10\kappa_{\rm in}$, respectively. See Sec. 3 for other parameters.

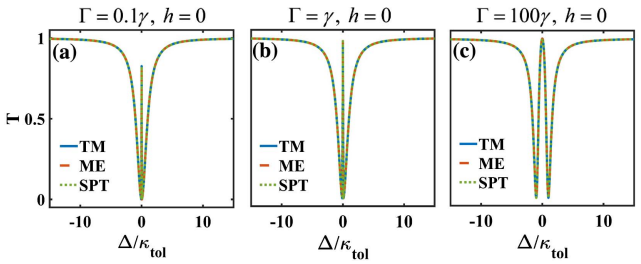

Fig. 3. Transmission spectra for a chiral QE-microresonator system without considering the backscattering: (a)–(c) $\Gamma = 0.1\gamma$, $\Gamma = \gamma$, and $\Gamma = 100\gamma$, respectively.

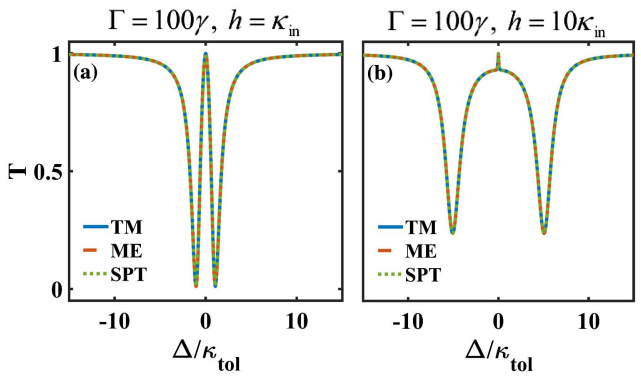

Fig. 4. Transmission spectra for a chiral QE-microresonator system with the QE and the scatterer: (a) $\Gamma = 100\gamma$, $h = \kappa_{\rm in}$ and (b) $\Gamma = 100\gamma$, h = $10\kappa_{\rm in}$.

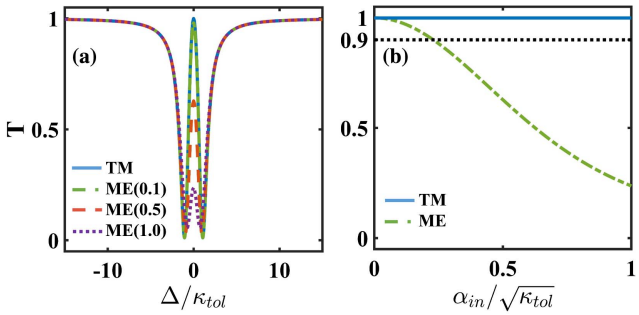

Fig. 5. (a) Transmission spectra for different driving amplitudes α_{in} (corresponding to different pump powers), where the blue solid curve is calculated by the TM method, and the green dash-dotted curve (the red dashed curve, the purple dotted curve) is calculated by the ME method, with $\alpha_{in}/\sqrt{\kappa_{tol}} = 0.1$ ($\alpha_{in}/\sqrt{\kappa_{tol}} = 0.5$, $\alpha_{in}/\sqrt{\kappa_{tol}} = 1$). (b) Transmission spectra as a function of α_{in} at different decay rates, where $\Gamma = \gamma$ (the blue solid curve) and $\Gamma = 100\gamma$ (the red dash-dotted curve) correspond to weak and strong coupling, respectively. Other parameters are $\kappa_{ex} = \kappa_{in} = 0.5\kappa_{tol}$, $\gamma/\kappa_{tol} = 1 \times 10^{-4}$, $g/\kappa_{tol} = 1$, and $h = \kappa_{in}$.

especially at the resonant frequency $\Delta/\kappa_{tol} = 0$; see Fig. 5(a). This is because the average photon number of the system reaches its maximum at the resonance, and it is no longer a single-photon case. Figure 5(b) shows the transmission spectra versus the driving amplitude α_{in} at $\Delta/\kappa_{tol} = 0$. The result of the TM method is constant because it is independent of α_{in}. In contrast, in the ME method, the transmission decreases as α_{in} increases for both strong and weak coupling of the QE. As shown in Fig. 5(b), in the range of $\alpha_{in}/\sqrt{\kappa_{tol}} \leq 0.23$, the transmission calculated by the ME method is greater than 0.9 (see the black dotted line). At this time, the result calculated by the TM method, $T \approx 1$, is almost consistent with it. For a larger pump power, the TM method is no longer accurate. It is worth noting that at off-resonance, the TM method is still valid, as shown in Fig. 5(a).

4. Conclusion

We demonstrate that a two-level QE can be treated as a single-photon phase-amplitude modulator in a chiral QE-microresonator system. Based on this, we can solve the SPT problem by the method of TM. Theoretical analyses confirm that the TM method is consistent with the ME and the SPT methods. Also, the results of numerical analysis prove the correctness of parameter relationships. Without loss of generality, the TM method can be extended to solve the single-photon transmission of any number of two-level QEs chirally coupled to multiple microresonators.

Acknowledgement

This work was supported by the National Key R&D Program of China (Nos. 2019YFA0308700, 2017YFA0303703, and 2017YFA0303701), the National Natural Science Foundation of China (Nos. 11874212 and 11890704), the Fundamental Research Funds for the Central Universities (No. 021314380095), and the Program for Innovative Talents and Entrepreneurs in Jiangsu (No. JSSCTD202138).

References

1. S. Haroche and J.-M. Raimond, *Exploring the Quantum: Atoms, Cavities, and Photons* (Oxford University, 2006).
2. J.-T. Shen and S. Fan, "Strongly correlated multiparticle transport in one dimension through a quantum impurity," Phys. Rev. A **76**, 062709 (2007).
3. T. S. Tsoi and C. K. Law, "Quantum interference effects of a single photon interacting with an atomic chain inside a one-dimensional waveguide," Phys. Rev. A **78**, 063832 (2008).
4. J.-T. Shen and S. Fan, "Theory of single-photon transport in a single-mode waveguide. I. Coupling to a cavity containing a two-level atom," Phys. Rev. A **79**, 023837 (2009).
5. O. O. Chumak and E. V. Stolyarov, "Phase-space distribution functions for photon propagation in waveguides coupled to a qubit," Phys. Rev. A **88**, 013855 (2013).
6. N. V. Corzo, J. Raskop, A. Chandra, A. S. Sheremet, B. Gouraud, and J. Laurat, "Waveguide-coupled single collective excitation of atomic arrays," Nature **566**, 359 (2019).
7. J. Tang, Y. Wu, Z. Wang, H. Sun, L. Tang, H. Zhang, T. Li, Y. Lu, M. Xiao, and K. Xia, "Vacuum-induced surface-acoustic-wave phonon blockade," Phys. Rev. A **101**, 053802 (2020).
8. S. Pucher, C. Liedl, S. Jin, A. Rauschenbeutel, and P. Schneeweiss, "Atomic spin-controlled non-reciprocal Raman amplification of fibre-guided light," arXiv:2107.07272 (2021).
9. C.-H. Yan, M. Li, X.-B. Xu, Y.-L. Zhang, H. Yuan, and C.-L. Zou, "Unidirectional transmission of single photons under nonideal chiral photon-atom interactions," Phys. Rev. A **102**, 053719 (2020).
10. L. Zhou, Z. R. Gong, Y.-X. Liu, C. P. Sun, and F. Nori, "Controllable scattering of a single photon inside a one-dimensional resonator waveguide," Phys. Rev. Lett. **101**, 100501 (2008).
11. C.-H. Yan, W.-Z. Jia, and L.-F. Wei, "Controlling single-photon transport with three-level quantum dots in photonic crystals," Phys. Rev. A **89**, 033819 (2014).
12. C.-H. Yan and L.-F. Wei, "Single photon transport along a one-dimensional waveguide with a side manipulated cavity QED system," Opt. Express **23**, 10374 (2015).
13. P. Yang, X. Xia, H. He, S. Li, X. Han, P. Zhang, G. Li, P. Zhang, J. Xu, Y. Yang, and T. Zhang, "Realization of nonlinear optical nonreciprocity on a few-photon level based on atoms strongly coupled to an asymmetric cavity," Phys. Rev. Lett. **123**, 233604 (2019).
14. E. V. Stolyarov, "Single-photon switch controlled by a qubit embedded in an engineered electromagnetic environment," Phys. Rev. A **102**, 063709 (2020).
15. X.-X. Hu, Z.-B. Wang, P. Zhang, G.-J. Chen, Y.-L. Zhang, G. Li, X.-B. Zou, T. Zhang, H. X. Tang, C.-H. Dong, G.-C. Guo, and C.-L. Zou, "Noiseless photonic non-reciprocity via optically-induced magnetization," Nat. Commun. **12**, 2389 (2021).
16. J. Tang, L. Tang, H. Wu, Y. Wu, H. Sun, H. Zhang, T. Li, Y. Lu, M. Xiao, and K. Xia, "Towards on-demand heralded single-photon sources via photon blockade," Phys. Rev. Appl. **15**, 064020 (2021).
17. L. Tang, J. Tang, H. Wu, J. Zhang, M. Xiao, and K. Xia, "Broad-intensity-range optical nonreciprocity based on feedback-induced Kerr nonlinearity," Photonics Res. **9**, 1218 (2021).
18. L. Wang and J. Shi, "Quantum fluctuation and interference effect in a single atom–cavity QED system driven by a broadband squeezed vacuum," Chin. Opt. Lett. **18**, 122701 (2020).
19. M. S. Tame, K. R. McEnery, Ş. K. Özdemir, J. Lee, S. A. Maier, and M. S. Kim, "Quantum plasmonics," Nat. Phys. **9**, 329 (2013).
20. J. D. Cox, M. R. Singh, M. A. Antón, and F. Carreño, "Plasmonic control of nonlinear two-photon absorption in graphene nanocomposites," J. Phys. Condens. Matter **25**, 385302 (2013).
21. V. F. Nezhad, C. You, and G. Veronis, "Nanoplasmonic magneto-optical isolator [Invited]," Chin. Opt. Lett. **19**, 083602 (2021).

22. G. Chen, J. Zhu, and X. Li, "Influence of a dielectric decoupling layer on the local electric field and molecular spectroscopy in plasmonic nanocavities: a numerical study," Chin. Opt. Lett. **19**, 123001 (2021).
23. M. R. Singh, G. Brassem, and S. Yastrebov, "Optical quantum yield in plasmonic nanowaveguide," Nanotechnology **32**, 135207 (2021).
24. B. Dayan, A. S. Parkins, T. Aoki, E. P. Ostby, K. J. Vahala, and H. J. Kimble, "A photon turnstile dynamically regulated by one atom," Science **319**, 1062 (2008).
25. T. Aoki, A. S. Parkins, D. J. Alton, C. A. Regal, B. Dayan, E. Ostby, K. J. Vahala, and H. J. Kimble, "Efficient routing of single photons by one atom and a microtoroidal cavity," Phys. Rev. Lett. **102**, 083601 (2009).
26. J.-T. Shen and S. Fan, "Theory of single-photon transport in a single-mode waveguide. II. Coupling to a whispering-gallery resonator containing a two-level atom," Phys. Rev. A **79**, 023838 (2009).
27. C. Junge, D. O'Shea, J. Volz, and A. Rauschenbeutel, "Strong coupling between single atoms and nontransversal photons," Phys. Rev. Lett. **110**, 213604 (2013).
28. Q.-T. Cao, H. Wang, C.-H. Dong, H. Jing, R.-S. Liu, X. Chen, L. Ge, Q. Gong, and Y.-F. Xiao, "Experimental demonstration of spontaneous chirality in a nonlinear microresonator," Phys. Rev. Lett. **118**, 033901 (2017).
29. R. Huang, A. Miranowicz, J.-Q. Liao, F. Nori, and H. Jing, "Nonreciprocal photon blockade," Phys. Rev. Lett. **121**, 153601 (2018).
30. E. Will, L. Masters, A. Rauschenbeutel, M. Scheucher, and J. Volz, "Coupling a single trapped atom to a whispering-gallery-mode microresonator," Phys. Rev. Lett. **126**, 233602 (2021).
31. P. Lodahl, S. Mahmoodian, S. Stobbe, A. Rauschenbeutel, P. Schneeweiss, J. Volz, H. Pichler, and P. Zoller, "Chiral quantum optics," Nature **541**, 473 (2017).
32. K. Xia, G. Lu, G. Lin, Y. Cheng, Y. Niu, S. Gong, and J. Twamley, "Reversible nonmagnetic single-photon isolation using unbalanced quantum coupling," Phys. Rev. A **90**, 043802 (2014).
33. I. M. Mirza, J. G. Hoskins, and J. C. Schotland, "Chirality, band structure, and localization in waveguide quantum electrodynamics," Phys. Rev. A **96**, 053804 (2017).
34. S. Barik, A. Karasahin, C. Flower, T. Cai, H. Miyake, W. DeGottardi, M. Hafezi, and E. Waks, "A topological quantum optics interface," Science **359**, 666 (2018).
35. L. Tang, J. Tang, W. Zhang, G. Lu, H. Zhang, Y. Zhang, K. Xia, and M. Xiao, "On-chip chiral single-photon interface: isolation and unidirectional emission," Phys. Rev. A **99**, 043833 (2019).
36. M. J. Mehrabad, A. P. Foster, R. Dost, E. Clarke, P. K. Patil, A. M. Fox, M. S. Skolnick, and L. R. Wilson, "Chiral topological photonics with an embedded quantum emitter," Optica **7**, 1690 (2020).
37. Y. Zhou, D.-Y. Lü, and W.-Y. Zeng, "Chiral single-photon switch-assisted quantum logic gate with a nitrogen-vacancy center in a hybrid system," Photonics Res. **9**, 405 (2021).
38. M. J. Mehrabad, A. P. Foster, N. Martin, R. Dost, E. Clarke, P. K. Patil, M. S. Skolnick, and L. R. Wilson, "A chiral topological add-drop filter for integrated quantum photonic circuits," arXiv:2110.07277 (2021).
39. C. Sayrin, C. Junge, R. Mitsch, B. Albrecht, D. O'Shea, P. Schneeweiss, J. Volz, and A. Rauschenbeutel, "Nanophotonic optical isolator controlled by the internal state of cold atoms," Phys. Rev. X **5**, 041036 (2015).
40. M. Scheucher, A. Hilico, E. Will, J. Volz, and A. Rauschenbeutel, "Quantum optical circulator controlled by a single chirally coupled atom," Science **354**, 1577 (2016).
41. Y. Kawaguchi, M. Li, K. Chen, V. Menon, A. Alù, and A. B. Khanikaev, "Optical isolator based on chiral light–matter interactions in a ring resonator integrating a dichroic magneto-optical material," Appl. Phys. Lett. **118**, 241104 (2021).
42. I. Söllner, S. Mahmoodian, S. L. Hansen, L. Midolo, A. Javadi, G. Kiršanskė, T. Pregnolato, H. El-Ella, E. H. Lee, J. D. Song, S. Stobbe, and P. Lodahl, "Deterministic photon-emitter coupling in chiral photonic circuits," Nat. Nanotechnol. **10**, 775 (2015).
43. S. Guddala, Y. Kawaguchi, F. Komissarenko, S. Kiriushechkina, A. Vakulenko, K. Chen, A. Alù, V. M. Menon, and A. B. Khanikaev, "All-optical nonreciprocity due to valley polarization pumping in transition metal dichalcogenides," Nat. Commun. **12**, 3746 (2021).
44. D. W. Vernooy, A. Furusawa, N. P. Georgiades, V. S. Ilchenko, and H. J. Kimble, "Cavity QED with high-q whispering gallery modes," Phys. Rev. A **57**, R2293 (1998).
45. R. Miller, T. E. Northup, K. M. Birnbaum, A. Boca, A. D. Boozer, and H. J. Kimble, "Trapped atoms in cavity QED: coupling quantized light and matter," J. Phys. B At. Mol. Opt. Phys. **38**, S551 (2005).
46. T. Aoki, B. Dayan, E. Wilcut, W. P. Bowen, A. S. Parkins, T. J. Kippenberg, K. J. Vahala, and H. J. Kimble, "Observation of strong coupling between one atom and a monolithic microresonator," Nature **443**, 671 (2006).
47. K. Srinivasan and O. Painter, "Mode coupling and cavity-quantum-dot interactions in a fiber-coupled microdisk cavity," Phys. Rev. A **75**, 023814 (2007).
48. K. Srinivasan and O. Painter, "Linear and nonlinear optical spectroscopy of a strongly coupled microdisk-quantum dot system," Nature **450**, 862 (2007).
49. A. Mazzei, S. Götzinger, L. de S. Menezes, G. Zumofen, O. Benson, and V. Sandoghdar, "Controlled coupling of counterpropagating whispering-gallery modes by a single Rayleigh scatterer: a classical problem in a quantum optical light," Phys. Rev. Lett. **99**, 173603 (2007).
50. J. T. Shen and S. Fan, "Coherent photon transport from spontaneous emission in one-dimensional waveguides," Opt. Lett. **30**, 2001 (2005).
51. J.-T. Shen and S. Fan, "Coherent single photon transport in a one-dimensional waveguide coupled with superconducting quantum bits," Phys. Rev. Lett. **95**, 213001 (2005).
52. H. Zheng, "Interacting photons in waveguide-QED and applications in quantum information processing," Ph.D. Thesis (Duke University, 2013).
53. D. G. Rabus, *Integrated Ring Resonators* (Springer, 2007).
54. M. Rosenblit, P. Horak, S. Helsby, and R. Folman, "Single-atom detection using whispering-gallery modes of microdisk resonators," Phys. Rev. A **70**, 053808 (2004).
55. F. Morichetti, A. Melloni, A. Breda, A. Canciamilla, C. Ferrari, and M. Martinelli, "A reconfigurable architecture for continuously variable optical slow-wave delay lines," Opt. Express **15**, 17273 (2007).
56. C. F. Andrea Melloni, Francesco Morichetti, and M. Martinelli, "Continuously tunable 1 byte delay in coupled-resonator optical waveguides," Opt. Lett. **33**, 2389 (2008).
57. J. K. Poon, L. Zhu, G. A. DeRose, and A. Yariv, "Transmission and group delay of microring coupled-resonator optical waveguides," Opt. Lett. **31**, 456 (2006).
58. F. Xia, L. Sekaric, and Y. Vlasov, "Ultracompact optical buffers on a silicon chip," Nat. Photonics **1**, 65 (2007).
59. M. Hafezi, S. Mittal, J. Fan, A. Migdall, and J. M. Taylor, "Imaging topological edge states in silicon photonics," Nat. Photonics **7**, 1001 (2013).
60. J. Wang, Z. Yao, and A. W. Poon, "Silicon-nitride-based integrated optofluidic biochemical sensors using a coupled-resonator optical waveguide," Front. Mater. **2**, 34 (2015).
61. M. Atatüre, J. Dreiser, A. Badolato, A. Högele, K. Karrai, and A. Imamoglu, "Quantum-dot spin-state preparation with near-unity fidelity," Science **312**, 551 (2006).
62. X. Xu, Y. Wu, B. Sun, Q. Huang, J. Cheng, D. G. Steel, A. S. Bracker, D. Gammon, C. Emary, and L. J. Sham, "Fast spin state initialization in a singly charged InAs-GaAs quantum dot by optical cooling," Phys. Rev. Lett. **99**, 097401 (2007).
63. X. Xu, B. Sun, P. R. Berman, D. G. Steel, A. S. Bracker, D. Gammon, and L. J. Sham, "Coherent population trapping of an electron spin in a single negatively charged quantum dot," Nat. Phys. **4**, 692 (2008).
64. K. Xia and J. Twamley, "All-optical switching and router via the direct quantum control of coupling between cavity modes," Phys. Rev. X **3**, 031013 (2013).
65. P. M. Vora, A. S. Bracker, S. G. Carter, T. M. Sweeney, M. Kim, C. S. Kim, L. Yang, P. G. Brereton, S. E. Economou, and D. Gammon, "Spin-cavity interactions between a quantum dot molecule and a photonic crystal cavity," Nat. Commun. **6**, 7665 (2015).
66. C.-K. Yong, J. Horng, Y. Shen, H. Cai, A. Wang, C.-S. Yang, C.-K. Lin, S. Zhao, K. Watanabe, T. Taniguchi, S. Tongay, and F. Wang, "Biexcitonic optical Stark effects in monolayer molybdenum diselenide," Nat. Phys. **14**, 1092 (2018).
67. J. D. Thompson, T. G. Tiecke, N. P. de Leon, J. Feist, A. V. Akimov, M. Gullans, A. S. Zibrov, V. Vuletić, and M. D. Lukin, "Coupling a single trapped atom to a nanoscale optical cavity," Science **340**, 1202 (2013).
68. D. E. Chang, J. S. Douglas, A. González-Tudela, C.-L. Hung, and H. J. Kimble, "Colloquium: quantum matter built from nanoscopic lattices of atoms and photons," Rev. Mod. Phys. **90**, 031002 (2018).
69. J. Yang, C. Qian, X. Xie, K. Peng, S. Wu, F. Song, S. Sun, J. Dang, Y. Yu, S. Shi, J. He, M. J. Steer, I. G. Thayne, B.-B. Li, F. Bo, Y.-F. Xiao, Z. Zuo, K. Jin, C. Gu,

and X. Xu, "Diabolical points in coupled active cavities with quantum emitters," Light Sci. Appl. **9**, 6 (2020).
70. Y.-M. He, G. Clark, J. R. Schaibley, Y. He, M.-C. Chen, Y.-J. Wei, X. Ding, Q. Zhang, W. Yao, X. Xu, C.-Y. Lu, and J.-W. Pan, "Single quantum emitters in monolayer semiconductors," Nat. Nanotechnol. **10**, 497 (2015).
71. A. Branny, S. Kumar, R. Proux, and B. D. Gerardot, "Deterministic strain-induced arrays of quantum emitters in a two-dimensional semiconductor," Nat. Commun. **8**, 15053 (2017).
72. C. Palacios-Berraquero, D. M. Kara, A. R. P. Montblanch, M. Barbone, P. Latawiec, D. Yoon, A. K. Ott, M. Loncar, A. C. Ferrari, and M. Atatüre, "Large-scale quantum-emitter arrays in atomically thin semiconductors," Nat. Commun. **8**, 15093 (2017).
73. M. Hafezi, E. A. Demler, M. D. Lukin, and J. M. Taylor, "Robust optical delay lines with topological protection," Nat. Phys. **7**, 907 (2011).
74. M. O. Scully and M. S. Zubairy, *Quantum Optics* (American Association of Physics Teachers, 1999).
75. F. Wolfgramm, "Atomic quantum metrology with narrowband entangled and squeezed states of light," Ph.D. thesis (Institut de Ciències Fotòniques, 2012).
76. J. Tang, W. Nie, L. Tang, M. Chen, X. Su, Y. Lu, F. Nori, and K. Xia, "Nonreciprocal single-photon band structure," arXiv:2111.06104 (2021).
77. F. Morichetti, C. Ferrari, A. Canciamilla, and A. Melloni, "The first decade of coupled resonator optical waveguides: bringing slow light to applications," Laser Photon. Rev. **6**, 74 (2012).